ASME Journal of Offshore Mechanics and Arctic Engineering
Online journal at:
https://asmedigitalcollection.asme.org/offshoremechanics

Serviceability Limit State Assessment of Semi-Submersible Floating Wind Turbines

Shuaishuai Wang[1]
Department of Marine Technology,
Norwegian University of Science and Technology (NTNU),
Trondheim 7491, Norway
e-mail: shuaishuai.wang@ntnu.no

Torgeir Moan
Department of Marine Technology,
Norwegian University of Science and Technology (NTNU),
Trondheim 7491, Norway;
Faculty of Maritime and Transportation,
Ningbo University,
Ningbo, China
e-mail: torgeir.moan@ntnu.no

The design of a floating wind turbine (FWT) should satisfy the serviceability limit state (SLS) requirement for an efficient and safe operation throughout the entire work life. The SLS requirements are introduced by the owner/developer of the wind turbine facility to achieve serviceability (production of power) or an efficient operation of the facility or a "first step" towards ensuring safety. Currently, there is limited information about SLS requirements in design standards. This study deals with an assessment of current methods, criteria, and procedure for the SLS design check with an emphasis on tilt/pitch and nacelle accelerations in view of power production and its fluctuations. Moreover, other criteria, on the borderline between serviceability and safety criteria, e.g., relating to clearance, are briefly discussed. The criteria relating to power production are illustrated in a case study with a 10-MW semi-submersible FWT considered for an offshore site in the Northern North Sea. Simplified static/dynamic analysis methods for use in the global design phase and high fidelity integrated, dynamic analysis methods for detailed design in terms of serviceability are presented, discussed, and applied in the case study. A good understanding of wind turbine dynamic performance associated with serviceability is essential to facilitate design decision-making. The relative contribution of wind and wave loads to the different SLS criteria is investigated. Finally, the main conclusions are summarized. In lieu of the current state of the art regarding SLS requirements for FWTs, we hope that this study provides a basis for improving design standards and guiding research and engineering practice for the semi-submersible floater design of FWTs. [DOI: 10.1115/1.4063618]

Keywords: serviceability, semi-submersible floater, floating wind turbine, static and dynamic analysis, tilt angle, nacelle acceleration., design of offshore structures, dynamics of structures, hydrodynamics, system integrity assessment

1 Introduction

Wind turbines have to be designed for serviceability and safety requirements. In general, quantitative requirements in terms of limit states are aimed at. Safety requirements include fatigue limit state (FLS), ultimate limit state (ULS), and accidental limit state (ALS) (damage tolerance) requirements.

While safety requirements established by regulatory bodies are mandatory for certification and e.g., insurance, serviceability requirements (limit states) are decided by the owner of the facility to achieve serviceability (production of power) or an efficient operation of the facility or a "first step" towards ensuring safety. Serviceability limit states (SLS) refer to conditions other than structural strength that render the structure or facility unusable. (SLS represents criteria governing normal functional or operational use). In general, SLS design of structures includes factors such as durability (by appropriate detailing to reduce corrosion and excessive wear), deflection/displacement, or accelerations that reduce the overall performance of the power production system (rotor, drivetrain), lubrication of rotational equipment, e.g., in the gearbox that may cause leakage, and excessive vibration (partly by limiting natural frequencies to avoid resonances). Serviceability requirements also include ease of maintenance and repair, to ensure: accessibility of structural parts for maintenance and inspection, renewal of corrosion protection, replacement of equipment, mooring lines and anchors, and cables with minimum disruption to the use of the structure. Such requirements are often formulated in a qualitative form.

The design process aims ideally at determining the facility that satisfies all the design criteria at the lowest lifecycle costs. Such a process is iterative and is conveniently split into initial design, pre-engineering and ends with a detailed design. This process, therefore, needs to start with a focus on determining the global layout before proceeding to local design. Moreover, the iterative approach is based on using an increasing refinement of methods, from initial design to detailed design. The serviceability criteria are mainly considered in the initial design phase for determining main global performance such as overall global dimensions of the floater and power generation. The initial design methodology for floating wind turbines is illustrated by Li et al. [1].

In the present paper, the focus is on serviceability performance relating to the power production and its variability, as measured in terms of the floater tilt angle and nacelle accelerations. It is

[1]Corresponding author.

Contributed by the Ocean, Offshore, and Arctic Engineering Division of ASME for publication in the Journal of Offshore Mechanics and Arctic Engineering. Manuscript received April 25, 2023; final manuscript received August 19, 2023; published online December 4, 2023. Assoc. Editor: Amy Robertson.

noted that the tilt is intimately connected to safety requirements through the requirements of intact stability. Some developers also consider the nacelle (rotor) acceleration measure as a safety precaution for the drivetrain. However, our opinion is that safety criteria both for the structure and drivetrain should be treated by explicit safety criteria and load effect analysis. Several important serviceability requirements are described and the main criteria are proposed. The SLS is checked for representative load cases with annual occurrence based on the environmental contour method covering the normal operating conditions and the parked condition. It is a common practice to assess the serviceability performance based on annual environmental conditions. The dynamic characteristics of the serviceability performance under turbulent wind and irregular wave loads are investigated. In addition, the floater tilt angle is estimated by a simplified analysis method in the global design and is compared to the realistic condition with the detailed fully coupled model. More details about the description of the criteria, methods, case study models, results, and main findings are presented in the following sections. Since the SLS information in the current wind turbine design codes is very limited, this study aims at shedding light on serviceability performance with respect to power generation. Moreover, we highlight other possible criteria, which require further development since they are on the borderline between serviceability and safety criteria.

2 Serviceability Limit States

It is noted that SLS criteria are not mandatory to follow. If they cannot be complied with during operation, they can be handled by operational criteria. For instance, if SLS requirements related to the power production phase cannot be complied with for certain environmental conditions, the system could be parked under such conditions and relaxed requirements will apply. However, this would imply a reduction in Annual Energy Production (AEP). Clearly, making serviceability criteria more restrictive might imply additional fabrication costs and, on the other hand, increase power production. Hence, it might be envisaged that serviceability criteria can be optimized.

In general, the criteria are formulated by quantitative measures of certain performance parameters. Serviceability refers to the use or operation of the facility. For the verification of various serviceability requirements, the characteristic or quasi-permanent combinations of loads are often applied for some serviceability constraints, taking into account the effects of short-term and long-term duration of loads and various design situations. Typically, serviceability criteria are formulated with reference to the annual occurrence of environmental conditions or loads. However, wind turbines are operated at given wind speeds, say, 4–5 to 25 m/s, and serviceability criteria should naturally refer to such wind conditions and the associated wave conditions.

As mentioned earlier, it is up to the owner/operator of the wind energy facility to determine the SLS criteria. As indicated below, several important SLS criteria refer to the rotor/drivetrain, and the manufacturer of such equipment also has a saying that should be reflected in the actual criteria used.

The design criteria are based on specified characteristic loads, safety factors and response (load effect) acceptance criteria. Traditionally, SLS criteria are based on partial safety factors equal to 1.0. Hence, the reliability level is defined by the characteristic loads and the load effect acceptance criteria. To illustrate the effect of the definition of characteristic loads, two sets of characteristic loads are considered: one based on most probable Hs, Tp conditional upon the wind speed; and one based on considerations of consistently defined conditions corresponding to an annual return period.

The following three examples of important serviceability requirements are briefly outlined, namely, tilt angle, nacelle acceleration, and clearances between structure/equipment and wave surface. Tentative criteria for the first two limit states are indicated.

2.1 Tilt Angle. The serviceability criterion relating to the tilt angle for bottom fixed wind turbines is normally based on the tolerance requirements specified by "turbine manufacturer." Ideally, these should be turbine specific, i.e., size and the hub height, with gearbox or direct drive. Sometimes, these tolerances are specified in some codes of practice (e.g., DNVGL-ST-0126 [2]). Some of the specific requirements are as follows:

- Maximum allowable rotation at pile head after installation.
- Maximum accumulated permanent rotation resulting from cyclic and dynamic loading over the design life.

With this background, it is interesting to notice that common practice is to allow a tilt of floating wind turbines in the range of 5–10 deg. The apparent inconsistency between criteria for fixed and floating turbines is difficult to understand. Clearly, a less stringent tilt criterion for bottom fixed wind turbines will reduce the foundation costs and installation time and costs.

In the global design phase, the static tilt angle can be estimated by static equilibrium consideration without accounting for the mooring restoring and satisfy a maximum of 8 deg tilt.

In detailed design, an integrated dynamic analysis, with a full account of the wind and wave loads and the effect of the mooring restoration. The following limits have been suggested:

- Maximum (steady) tilt during selected operational load cases (e.g., IEC design load case (DLC) 1.6 [3]) is limited to 5 deg (mean value of the time series) and Maximum combined tilt and pitch/roll angle 10 deg (max. value in the time series).
- Maximum combined tilt and pitch/roll angle during non-operational load cases (e.g., IEC DLC6.3 [3]) is limited to 15 deg (max. value in the time series). The angle can be measured at the top of the tower and includes elastic deformations of the tower.

2.2 Maximum Acceleration of the Nacelle. In the conceptual design phase, the acceleration of the nacelle might be estimated by a simplified dynamic analysis, focusing on selected wave conditions. This analysis can be based on the response amplitude operator (RAO) of the nacelle acceleration.

In detailed design, based on a fully integrated analysis, the following maximum acceleration limits might then be applied:

- Maximum acceleration during operational load cases (e.g., IEC DLC1.6 [3]) is limited to 0.3 g (max. value in the time series), where g is the acceleration of gravity.
- Maximum acceleration during the parked condition (e.g., IEC DLC6.3 [3]) is limited to 0.6 g (max. value in the time series).

It is noted that in the present work, only nacelle surge accelerations are assessed referring to the above criteria, while side–side and vertical parts due to nacelle sway, heave, and pitch accelerations might be considered in the detailed design, by communicating with wind turbine companies.

In addition, the limitations to tilt and nacelle acceleration are especially meant to refer to the performance of the rotor-nacelle assembly (RNA). It has been demonstrated in the study by Nejad et al. [4] that the acceleration level only partially reflects the forces and moments and the corresponding bearing loads, etc., in the drivetrain. Hence, the criteria relating to the RNA could be assessed in more detail for the operation and transport/installation of the RNA. Also, tuning the controller might be an issue in resolving any non-compliance with the criteria during the operation.

It shall be discussed whether serviceability criteria need to be fulfilled for operational conditions with fault (such as DLCs 2.1 and 2.3). We have omitted this because the faulted conditions might be related to the safety criteria. In addition, it is not quite clear whether the SLS assessment for parked conditions is required; still, this work includes an analysis of the parked conditions to shed light on the dynamic characteristics of the SLS performance and the importance of the load cases.

2.3 Discussion About the Possible Other Serviceability Limit States Criteria. In addition to the explicit serviceability criteria of the tilt angle and maximum acceleration of the nacelle, other criteria like wave clearance with respect to the air gap and freeboard in principle shall be determined according to the IEC standard 61400-3-2 [5] and the DNV standard 0119 [6], and they could be considered to be serviceability criteria. However, the following discussion suggests that they are more related to safety criteria, which are more restrictive.

In principle, if the airgap criterion is not fulfilled, satisfactory safety can be achieved by designing the structure to sustain the corresponding loads due to wave contact with the structure. A similar mitigation of the risk does not seem to exist in connection with freeboard. For instance, if a part of the hull is submerged, the result can be a serious loss of buoyancy and restoration and hence stability.

Hence, in the conceptual design, the freeboard should be justified by the determination of the static heeling position and a "conservative "margin of the freeboard, which indirectly conservatively account for the relative motions that can result in submergence or flooding of a buoyant part. (It is noted that a short, temporary submergence might not be critical, but this needs to be justified by integrated dynamic analysis.)

In the detailed design, the air gap and freeboard should be determined by relative motion analysis. Criteria with respect to the mean wave condition and steady floating position as well as the instantaneous relative position of the wave surface and the reference structural part should be considered for freeboard design.

It is seen that the clearance features relating to airgap and freeboard have a link to safety criteria, which primarily should be based on loads with a 50-year return period. As a conclusion, we consider clearance criteria, such as freeboard and air gap, as safety criteria and outside the scope of this paper. However, it is crucial to establish improved research-based safety criteria for clearance, such as air gap and freeboard.

2.4 Remarks on the Specification of Serviceability Limit States Criteria. Serviceability refers to the accumulated time where service (or functionality) can be maintained. Hence, the definition of which response variable to use to specify SLS requirements needs to be discussed. Using the long-term extreme value as the characteristic value would imply that the percentage of unserviceability will be very small.

In the present study, the "long-term" maxima for the operational and parked conditions are applied, in a simplified manner by using representative short-term conditions. The specification of the characteristic value should be further elaborated upon.

3 Description of Floater Concept and Wind Turbine Numerical Model for the Case Study

In this section, the main configuration and layout of the floater are introduced, which are closely linked to the serviceability performance. In addition, a fully coupled numerical model of the 10-MW floating wind turbine (FWT) is described, which is used to obtain the dynamic analysis results. More details are shown in Secs. 3.1 and 3.2, respectively.

3.1 Semi-Submersible Hull Concept. The main configuration of the semi-submersible hull refers to OO-Star [7] and CSC [8] floaters, which consist of four columns and three pontoons without braces/trusswork. The outer columns connect the central column through the three pontoons, and the turbine is mounted on the central column. The main layout and specifications of the hull are determined from a global conceptual design conducted by Li et al. [1]. The conceptual design study outlined a global conceptual design methodology and procedure for semi-submersible floaters and applied it to the 10-MW FWT. The conceptual design checks are based on criteria of serviceability, motion natural period, and intact stability. In addition, the dynamic performance of the hull global motions, accelerations, and internal loads in wave conditions is used as an assessment for choosing the hull layout and global dimensions.

In the conceptual design study, a simplified serviceability criterion is considered, which limits the static heeling angle under the maximum mean thrust force of the wind turbine in a free-floating mode within the range of 5–10 deg. However, it is also indicated that the mooring system has a large influence both on the heeling moment (lever) and the righting moment of the floater, thereby the heeling angle. A realistic tilt angle and the resultant power performance can be obtained from the dynamic analysis of the floating wind turbine under the moored condition.

The layout of the semi-submersible hull is shown in Fig. 1. Detailed global dimensions, mass, and hydrodynamic properties are presented in the technique report [9].

3.2 Fully Coupled Wind Turbine Numerical Model. A fully coupled aerohydroservoelastic FWT numerical model is established using SIMA (version 4.1.0), a simulation and analysis tool developed by SINTEF Ocean for marine operations and floating systems. The fully coupled numerical model of the 10-MW FWT is illustrated in Fig. 2.

The semi-submersible hull is modeled as a rigid body, while blades, tower, and shaft are modeled by using beam elements, and mooring lines are modeled by using bar elements. Nonlinear time domain analysis of the fully coupled model is carried out to obtain the dynamic load effects of rigid bodies and flexible structures.

Aerodynamic loads on blades are calculated based on the blade element momentum (BEM) method. Moreover, the wind drag force on the tower is estimated by the drag term of Morison's Formula [11] with a non-dimensional drag coefficient of 0.8. The hydrodynamic loads on the semi-submersible hull include the first-order and second-order wave excitation, wave radiation, and restoring loads, as well as the wave viscous loads. The second-order wave excitation force is important in estimating floater and thus nacelle

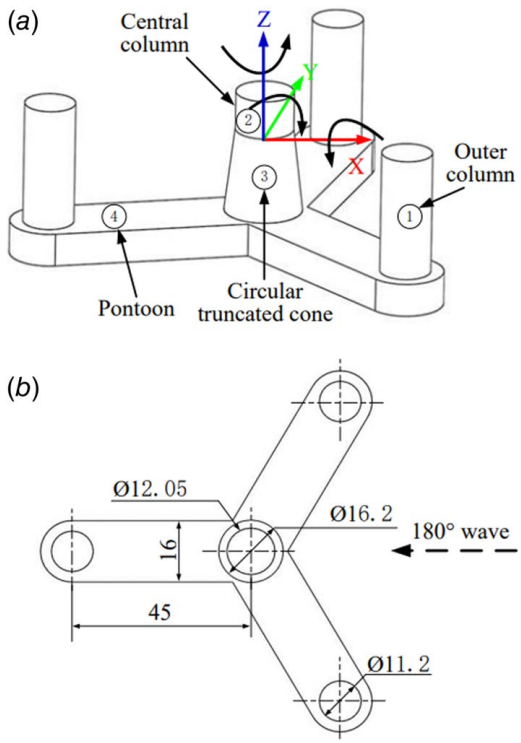

Fig. 1 Sketch of the 10-MW steel semi-submersible hull [10]: (*a*) main view and (*b*) top view

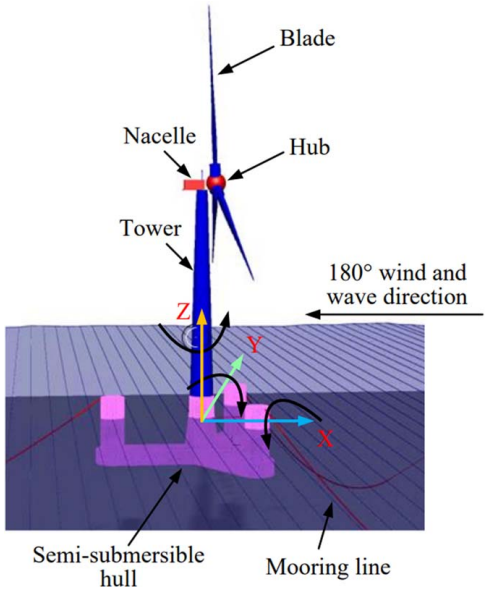

Fig. 2 Fully coupled numerical model of the 10-MW FWT

motions and accelerations [12], which is calculated using the full quadratic transfer function (QTF) approach. The first three items are calculated based on the potential flow theory, while the last one is estimated by the drag term of Morison's Formula [11] with coefficients on the hull as used in the LIFES 50+ project [7]. The controller system adopted is also used for the OO-Star 10-MW FWT model in the LIFES 50+ project [7], including features to avoid the negative damping effects in the FWT.

The main properties and characteristics of the 10-MW numerical wind turbine system are listed in Table 1. More detailed parameters can be found in the technical report [9].

4 Static and Dynamic Analysis of Serviceability Performance

4.1 Environmental Conditions. The environmental conditions are selected from an offshore location in the Northern North Sea. The hindcast data from 2001 to 2010 from the North Sea at offshore site 14 are used to generate wind and wave statistics. Then, a long-term joint wind and wave distribution is developed based on the one-hour mean wind speed at 10 m height above the mean sea level (U_{10}), significant wave height (Hs), and wave spectral peak period (Tp). A detailed description of the environmental data and the joint distribution can be found in the study by Li et al. [13].

Table 1 Main properties and characteristics of the 10-MW numerical wind turbine system

Parameter	Value
Rated power (MW)	10
Cut-in, rated and cut-out wind speed (m/s)	4, 11.4, 25
Nacelle height (m)	115.63
Water depth (m)	93
Fairlead vertical position above MSL (m)	11
Fairlead radial spacing (m)	50.6
Fairlead pretension (N)	2.0e6
Fairlead angle from MSL (deg)	27
First fore–aft natural frequency (Hz)	0.705
First side–side natural frequency (Hz)	0.725
Second fore–aft natural frequency (Hz)	2.437
Second side–side natural frequency (Hz)	2.107
Natural frequency in the surge, sway, heave, roll, pitch, and yaw (Hz)	0.0123, 0.0122, 0.0415, 0.0342, 0.0342, 0.0146

The load cases used in the dynamic analysis of Sec. 4 are summarized in Table 2. The mean wind speed at hub height covers normal operating conditions ranging from below-rated rated, to cut-off, and the parked condition. It is noted that both LC3 and LC4 are categorized into the rated condition since the mean wind speeds are very close. In each normal operating condition, the most probable Hs and Tp are selected according to the conditional distributions for a given U_{10}. The load case of the parked condition is selected with the maximum Hs on the 50-year contour surface.

In each load case, turbulent wind and irregular waves are used in the time domain dynamic simulations. The turbulence intensity (TI) used is that for the category of wind turbine Class C. The wind speed profiles follow the power law formulation with an exponent of 0.14. The Kaimal turbulence model and the JONSWAP spectrum are used to generate wind fields and irregular waves in time series, respectively.

Each simulation is executed for 4000 s with the time-step of 0.005 s, and the first 400 s are removed to avoid the transient effect. Thus, one-hour data are formed for response statistics analysis. In Sec. 4, only one sample is considered because the purpose is to reveal the characteristics of the serviceability performance under wind and wave loads rather than to evaluate the accurate extreme values.

4.2 Serviceability Performance Under Wind and Wave Loads

4.2.1 Combined Wind and Wave Conditions. Table 3 lists the mean values and standard deviations of the floater tilt angle, nacelle surge, and pitch accelerations under different wind and wave combined conditions.

As the load cases vary from LC1 to LC10, wind thrust force increases first and then tends to decrease, and the peak is located at the rated condition (LC3). In contrast, significant wave height and wave spectra peak period increase monotonously. It is found that large mean values and standard deviations of the floater tilt angle are located at the near-rated conditions. This implies that wind loads dominate the floater tilt angle. Second-order wave loads have a very small influence on the mean values of tilt/pitch angle, while the standard deviation is increased by almost 10% around the rated condition, and it generally increases from the rated to cut-out conditions. In contrast, both the mean value and standard deviation are influenced significantly by the second-order wave loads in the parked condition, reaching more than 15%.

Since the mean values of the nacelle surge and pitch accelerations are approximately zero, only standard deviations are shown in Table 3. Significant responses of the nacelle surge acceleration appear in the conditions LC7–LC11 and increase with the wave loads, implying that wave loads contribute significantly to the nacelle surge acceleration. In the critical load case range of LC7–

Table 2 Environmental conditions and load cases for operation and parked conditions

Condition	Load cases	U_{hub} (m/s)	T_I	Hs (m)	Tp (s)
Below-rated	LC1	8	0.174	1.9	9.7
	LC2	10	0.157	2.1	9.9
Rated	LC3	11.4	0.149	2.4	10.0
	LC4	12	0.146	2.5	10.1
Above-rated	LC5	14	0.138	2.8	10.3
	LC6	16	0.132	3.2	10.7
	LC7	18	0.127	3.6	10.9
	LC8	20	0.124	4.1	11.2
	LC9	22	0.121	4.6	11.5
Cut-out	LC10	24	0.118	5.4	11.9
Parked	LC11	45.2	0.112	15.4	14.5

Table 3 Response statistics of floater tilt/pitch, nacelle surge and pitch accelerations under different wind and wave combined conditions based on a single sample of 1 h

	Tilt/pitch (deg)						Nacelle surge acc. (m/s^2)			Nacelle pitch acc. (rad/s^2)	
	First		First + Second		%difference						
Load case	Mean	STD	Mean	STD	Mean	STD	First STD	Fir. + Sec. STD	%difference STD	First STD	Fir. + Sec. STD
LC1	2.34	0.58	2.33	0.64	−0.43	10.34	0.18	0.24	33.33	0.01	0.01
LC2	3.52	0.86	3.51	0.93	−0.28	8.14	0.20	0.25	25.00	0.01	0.01
LC3	3.51	0.92	3.50	1.02	−0.28	10.87	0.22	0.26	18.18	0.01	0.01
LC4	3.27	1.01	3.26	1.09	−0.31	7.92	0.23	0.27	17.39	0.02	0.02
LC5	2.65	0.98	2.63	1.05	−0.75	7.14	0.25	0.27	8.00	0.02	0.02
LC6	2.32	0.72	2.30	0.80	−0.86	11.11	0.26	0.28	7.69	0.02	0.02
LC7	2.11	0.60	2.09	0.68	−0.95	13.33	0.28	0.29	3.57	0.02	0.02
LC8	1.98	0.58	1.96	0.66	−1.01	13.79	0.30	0.31	3.33	0.02	0.02
LC9	1.90	0.57	1.87	0.65	−1.58	14.04	0.32	0.34	6.25	0.02	0.02
LC10	1.85	0.58	1.82	0.68	−1.62	17.24	0.35	0.37	5.71	0.02	0.02
LC11	1.03	1.16	0.88	1.38	−14.56	18.97	0.63	0.67	6.35	0.01	0.01

Note: "First" means only the first-order wave loads are considered; "First + second/Fir. + Sec." represents both the first- and second-order wave loads are considered. %difference = (Value (first + second)–Value(first))/Value(first)*100%.

LC11, second-order wave loads make the standard deviations of the nacelle surge accelerations increase by 3–6%. It is noted that a large difference due to the second-wave loads exists in low wind speed conditions, which is because the relative contribution of the first-order wave loads to the nacelle surge acceleration is small, while assessment of the response should be based on absolute values, which will be more critical in large wave conditions.

In contrast, the nacelle pitch acceleration in the parked condition is minimal compared to the normal operation condition. In normal operating conditions, the nacelle pitch acceleration increases with the load cases, and significant responses are located at the above-rated conditions. This implies that wind loads are the main cause of the nacelle pitch acceleration rather than the wave loads. It seems that the aerodynamic bending moment is the main cause of the nacelle pitch acceleration because it increases approximately with the mean wind speed, as shown in the study of Wang et al. [14].

Moreover, this is because the pitch acceleration is dominated by the response at high-frequency tower vibration resonance, as shown in Fig. 3(*c*), and the response is most likely caused by the aerodynamic bending moments. The second-order wave loads have very limited influence on the nacelle pitch accelerations, thereby the corresponding vertical accelerations because they are mainly induced by the wind loads. It is noted that the values of nacelle pitch accelerations are used to illustrate the dynamic characteristics in different load cases, and they should be transformed into translational accelerations with a rotation center of the nacelle system for serviceability assessment.

Dynamic characteristics of the floater tilt angle, and nacelle surge and pitch accelerations in different wind and first-order wave conditions are revealed by power spectra analysis, as shown in Fig. 3. In normal operating conditions, variation of the floater tilt angle is mainly caused by the low-frequency turbulent wind loads and response at the global pitch motion natural period. The global pitch motion resonance is mainly caused by wind loads because the response at the parked condition, where the wave loads are significant, is very limited, and the peaks are very sensitive to the load cases with varying wind load conditions. In the parked condition, wave loads mainly induce the variation of the floater tilt angle.

Nacelle surge acceleration mainly consists of three contributions, namely, wave loads induced response (global rigid motion acceleration in surge), global rigid motion acceleration in pitch, and response at the tower's first natural frequency. In both the normal operating and parked conditions, global rigid motion acceleration in pitch dominates the responses of the nacelle surge acceleration because of the large nacelle height. The global rigid motion acceleration in the surge is mainly induced by wave loads because the peaks increase with the wave loads from LC7 to LC11. The dynamic characteristics of the global floater motion acceleration in pitch are illustrated by the response amplitude operators (RAOs) for wave loads, which can be found in the technical report [9].

In normal operating conditions, the nacelle pitch acceleration is significant, which mainly consists of response contributions of wave loads, rotor 3P aerodynamic loads, and tower first and second resonance, where the tower second elastic resonance dominates.

4.2.2 Response in the Separate and Combined Wind and Wave Conditions. To get better insight into the contributions of wind and wave loads on the dynamic responses of floater tilt angle, and nacelle surge and pitch accelerations, the responses under wind and wave loads are studied separately. Figure 4 compares the mean values and standard deviations of the floater tilt angle, nacelle surge, and pitch accelerations between conditions only wind, only wave, and combined wind and wave loads.

In normal operating conditions, both mean values and standard deviations of the floater tilt angle for "wind + wave" and "only wind" conditions are very close. In the parked condition, the mean values are relatively small; in contrast, the standard deviations are significant. The conditions of "wind + wave" and "only wave" have very close standard deviations. The results indicate that the floater tilt angle can be estimated by only considering wind and wave loads for normal operating conditions and the parked condition, respectively.

In normal operating conditions, the standard deviation of nacelle surge acceleration in the "wind + wave" condition is obviously larger than those in "only wind" and "only wave" conditions. This means that both wind and wave loads contribute significantly to the nacelle surge acceleration, and combined wind and wave loads should be considered. In contrast, in the parked condition, responses of the nacelle surge acceleration in "wind + wave" and "only wave" conditions are very close; thus, the response can be estimated by only considering the wave loads. For the nacelle pitch acceleration, wind loads dominate in the normal operating conditions, while both wind and wave loads should be considered in the parked condition.

In Fig. 5, power spectra of the floater tilt angle, and nacelle surge and pitch accelerations are compared for conditions of "only wind", "only wave," and "wind and wave" loads. Two representative load cases of LC4 and LC11 are considered to illustrate the dynamic characteristics in the normal operating conditions and the parked condition, respectively.

For the floater tilt angle, in the LC4 condition, significant responses are located at the frequencies of turbulent wind and

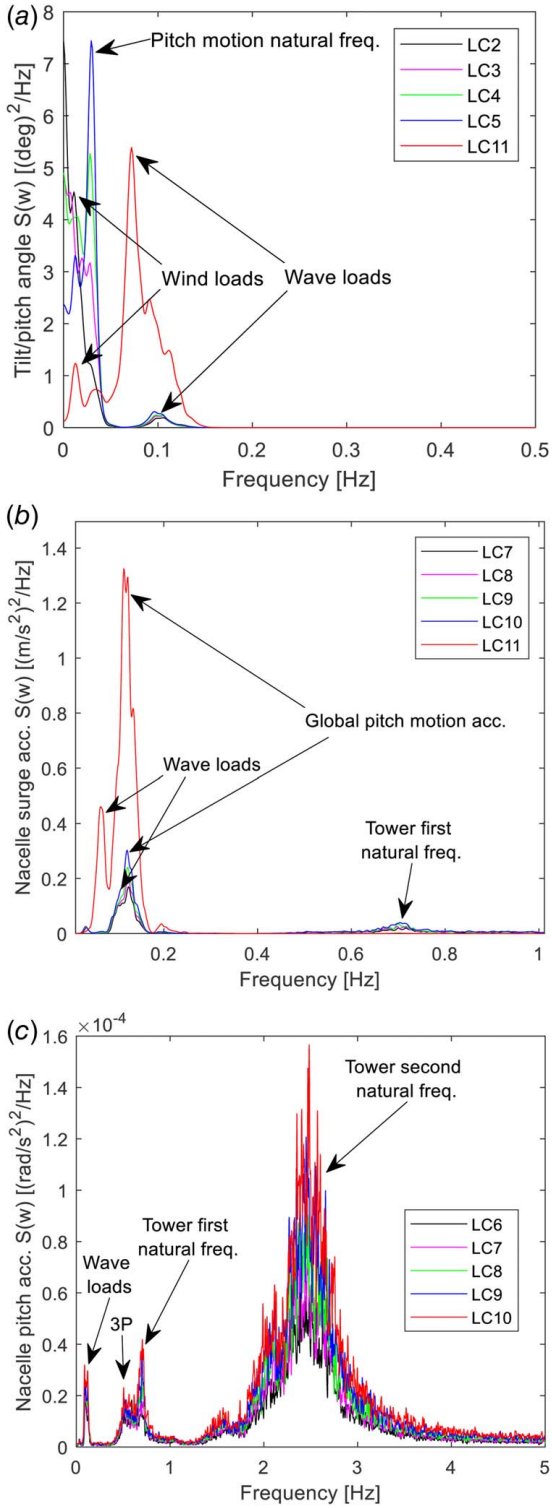

Fig. 3 Comparison of power spectra of floater tilt angle, and nacelle surge and pitch accelerations under different load cases, considering first-order wave loads only: (*a*) floater tilt angle, (*b*) nacelle surge acceleration, and (*c*) nacelle pitch acceleration.

global pitch motion resonance, and both are induced by wind loads. In contrast, in the LC11 condition, significant responses are caused by wave loads.

For the nacelle surge acceleration, in the LC4 condition, the main responses include the contributions of the global pitch motion resonance induced by wind loads, wave loads, and global pitch accelerations induced by wave loads, and tower first resonance induced by wind loads; the most significant responses are induced by the wave loads and global pitch accelerations due to the wave loads. It is emphasized that the response at the wave frequency include contributions of global surge and pitch motion accelerations induced by main wave energy. In contrast, the response of "Global pitch motion acceleration" is formed at the critical Tp condition where the RAO reaches the peak, as illustrated in Fig. 9. In the LC11 condition, since the wave loads are significant compared to the wind loads, the responses of the nacelle surge acceleration are mainly induced by wave loads. More specifically, the responses of the nacelle surge acceleration are primarily contributed by the wave loads and global pitch motion accelerations.

For the nacelle pitch acceleration, in the LC4 condition, the main responses are caused by the tower's first and second vibration resonance, and aerodynamic 3P excitation loads, which are induced by wind loads. In contrast, wave-induced responses are very limited. In the LC11 condition, the main responses are caused by wave loads and global pitch accelerations due to the wave loads, and the wind loads induced tower vibration resonance is minimal.

4.3 Static and Dynamic Tilt Angle Comparisons. In this section, the tilt angles of the floater estimated in the static and dynamic analyses are compared. The static tilt angle is calculated under the maximum mean thrust force of the wind turbine in a free-floating mode, which is expressed as follows:

$$\theta = \frac{M}{C_{55}} \tag{1}$$

where M presents the overturning moment, C_{55} is the hydrostatic stiffness in pitch (or roll) that is calculated by the Sesam module Wadam. The formulation for calculating the C_{55} is shown in the technical report [9] with a detailed description and the value for the floater in the present study is 1.67e9 Nm/rad.

Two parts of the overturning moment are considered: (1) the values caused by the rotor thrust force, and (2) the values induced by tower drag forces. The formulation is given as follows:

$$M = F_T \cdot H_h + \sum_{i=1}^{27} F_i \cdot H_i \tag{2}$$

where F_T is the rotor thrust force, H_h is the vertical distance between the hub center and the center of the floatation of the hull. F_i represents aerodynamic drag loads on the ith section of the tower. H_i presents the vertical distance between the center of the ith section of the tower and the center of the floatation. The tower drag forces are estimated by Morison's formula, and the total bending moment induced by the tower drag forces is about 3.03e6 Nm in the rated condition [15]. The maximum mean thrust force occurs at the LC3 (rated operating condition), and the value is about 1.24e6 N, as estimated from the one-hour dynamic responses of the FWT. The overturning moment for static tilt angle calculation is based on the floater in a vertical position, which will lead to a conservative result because the overturning moment will decrease when the tilt angle increases.

The tilt angle in the dynamic condition is estimated by the time domain analysis for the fully coupled FWT model with a detailed catenary mooring system, as illustrated in Fig. 2. The mooring system has a large influence both on the heeling moment due to the shorter arm and on the righting moment through the restoring effect. Therefore, a smaller tilt angle will be obtained in the moored condition compared to the free-floating condition. It is interesting to compare the realistic tilt angle estimated by the dynamic analysis for the fully coupled FWT model with the static tilt angle in view of the serviceability requirement. The comparison can provide a basis for improving the serviceability criterion.

Another aspect related to the tilt angle estimation for the serviceability analysis is the estimation of the thrust force, specifically whether it should be based on the onshore or floating offshore turbines. In fact, the serviceability design criterion is mainly used in

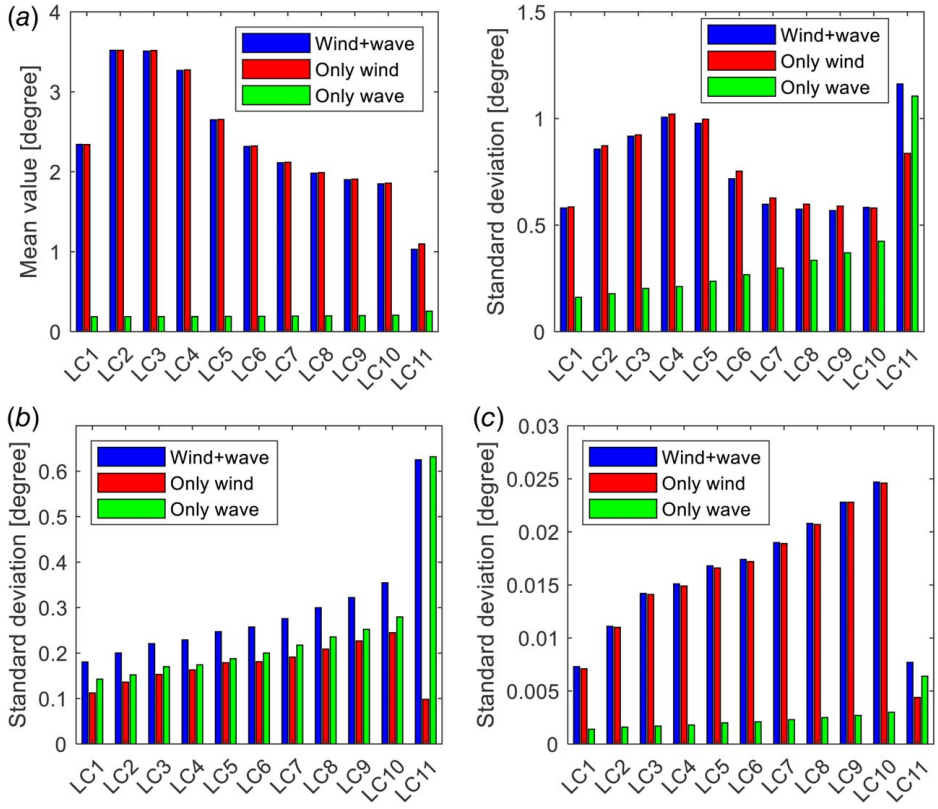

Fig. 4 Comparison of response statistics of floater tilt angle, and nacelle surge and pitch accelerations between conditions only wind loads, only wave loads, and combined wind and wave loads, considering first-order wave loads only: (*a*) mean value and STD of floater tilt/pitch angle, (*b*) STD of nacelle surge acceleration, and (c) STD of nacelle pitch acceleration

the floater global design stage, which usually refers to an original land-based turbine. Due to the change of controller system, the FWT and land-based turbine will produce different thrust forces, which will result in different tilt angles and, therefore, the serviceability performance.

Based on the earlier considerations, the static tilt angles estimated under the wind thrust forces of the land-based and floating offshore wind turbines, and the mean tilt angles in the dynamic condition are compared, as shown in Table 4. Due to the mooring system effect, the realistic tilt angle in the dynamic condition is around 30% smaller than in the static free-floating condition. The results give an indication of the possible improvement of the design practice in connection with the serviceability requirement. In addition, since the thrust force for the land-based turbine is larger than that of the floating one, the resulting tilt angle is also larger, which leads to a conservative serviceability performance. However, the difference in the static tilt angle depends very much on the controller design and turbine capacities; thus, a more general conclusion can be obtained by considering more cases to quantify this difference.

4.4 Nacelle Surge Acceleration Under Different Tp. The power spectra in Figs. 5(*c*) and 5(*d*) show that wave loads and pitch motion accelerations due to wave loads contribute significantly to the nacelle surge acceleration. It is straightforward to recognize that the nacelle surge acceleration will increase with significant wave height Hs. In this section, the effect of Tp on nacelle surge accelerations is investigated. A reference load case LC10 is used to conduct the case study because it causes the largest surge acceleration among the normal operating conditions.

Figure 6 presents the conditional distribution of Tp for given $U =$ 24 m/s and Hs = 5.4 m in LC10, showing a Tp range from 6 to 20 s. A total of 6 cases with Tp varying from 6 s to 16 s with an interval of 2 s are considered for conducting the dynamic simulations with the fully coupled FWT model. Figure 7 compares the standard deviations of the nacelle surge acceleration for the six Tp cases in the LC10. It shows that Tp has a large influence on the nacelle surge acceleration, and the most significant response occurs at the condition of Tp = 8 s.

Figure 8 illustrates the power spectra of the nacelle surge acceleration for different Tp cases under LC10, which aims to reveal the reason for the different responses. An obvious observation is that a significant peak appears in the case of Tp = 8 s, which is much larger than those of other Tp cases. The peak is located at the frequency of the global pitch motion acceleration of the floater. Figure 9 illustrates the RAOs of the pitch motion accelerations of the floater under wave loads, which shows a significant peak located at the frequency of 0.12 Hz. The wave excitation load period of 8 s approximates the characteristic period in the RAOs; therefore, the global pitch acceleration of the floater contributes to the nacelle surge acceleration significantly and this is due to the large tower height. The analysis implies that Tp significantly influences the nacelle surge acceleration, and RAO analysis of floater pitch acceleration under wave loads should be conducted to find the critical Tp for SLS assessment.

5 Case Study: Serviceability Limit States Assessment Under Annual Occurrence of Environmental Conditions

This section shows a procedure for the SLS assessment of FWTs. An application on the case study of the 10-MW semi-submersible FWT at offshore site 14 in the North Sea is illustrated.

5.1 Selection of Important Environmental Conditions. First, the annual occurrence of environmental conditions of the offshore site 14 is formulated. Figure 10 shows the 1-year

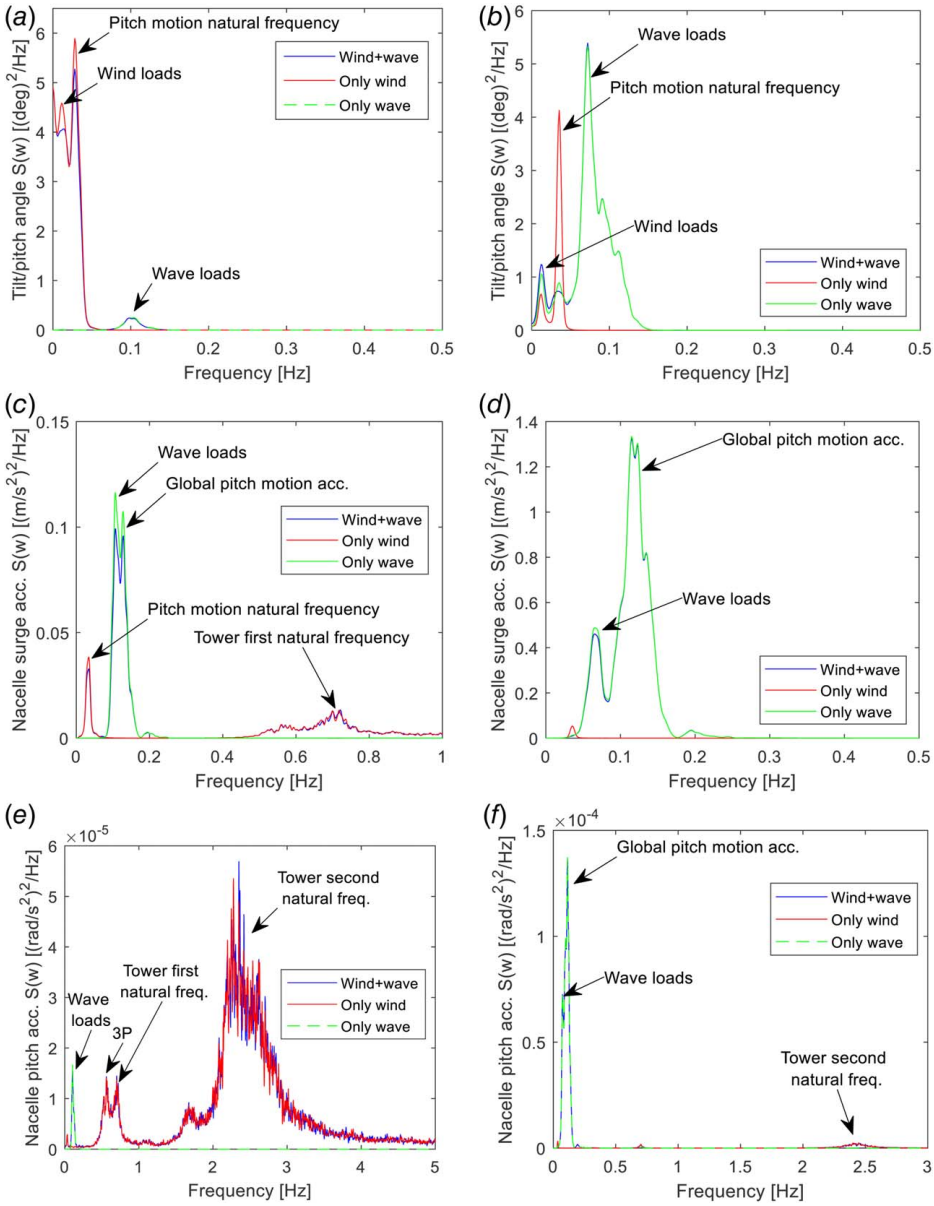

Fig. 5 Comparison of power spectra of floater tilt angle, and nacelle surge and pitch accelerations between conditions only wind loads, only wave loads, and combined wind and wave loads, considering first-order wave loads only: (*a*) tilt/pitch angle under LC4, (*b*) tilt/pitch angle under LC11, and (*c*) nacelle surge acceleration under LC4, (*d*) nacelle surge acceleration under LC11, (*e*) nacelle pitch acceleration under LC4, and (*f*) nacelle pitch acceleration under LC11

environmental contour surface obtained based on the joint distribution consisting of the marginal distribution of U10, the conditional distribution of Hs for given U10, and the conditional distribution of Tp for given both U10 and Hs, which are formulated in the study of Li et al. [13]. Based on the dynamic analysis in Sec. 5, the rated, cut-out, and parked conditions are found to be critical for SLS performance, which are, therefore, considered in the case study to simplify the load cases. Figure 11 shows the 1-year environmental contour lines of Hs–Tp for given mean wind speed at the hub for rated, cut-out, and two parked conditions. Noted that several parked contour lines exist, but only the following two with high mean wind speeds and large Hs are selected because of the large severity.

Table 4 Comparison of tilt angles between static and dynamic conditions, and between land-based and floating wind turbines

Condition	Tilt angle (deg)
Static condition: free-floating, FWT thrust force, tower drag force	Static tilt angle: 5.01
Static condition: free-floating, land-based turbine thrust force, tower drag force	Static tilt angle: 6.04
Dynamic condition: catenary mooring condition, FWT thrust force, tower drag force, wave loads	Mean value of dynamic tilt angle: 3.52

Each contour line contains many combinations of Hs–Tp that potentially cause the largest responses, where the most critical ones are selected for simulations, which are listed in Table 5. The selected environmental conditions are primarily based on the critical Tp and Hs that are closely associated with the tilt/pitch angle of the floater and nacelle surge accelerations. For instance, in the contour line (a) rated condition, EC1–1 is selected with the critical Tp value that approximates 8.3 s, which is significant in estimating nacelle

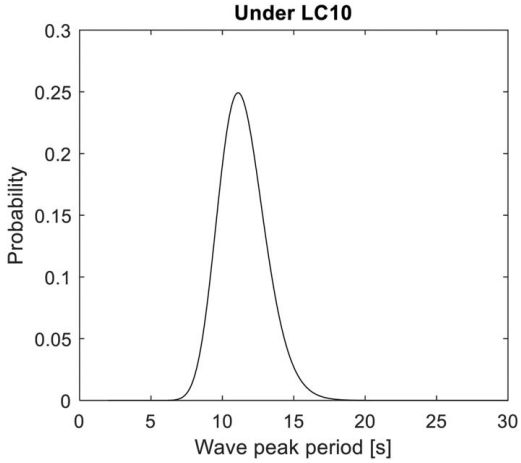

Fig. 6 Conditional distribution of wave spectra peak period Tp for given mean wind speed U and significant wave height Hs under LC10

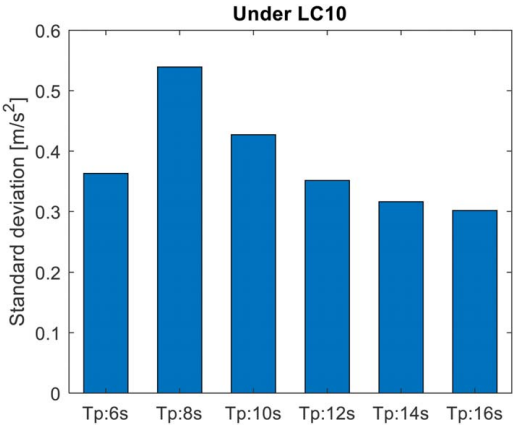

Fig. 7 Standard deviations of nacelle surge acceleration for different Tp under LC10

surge acceleration, as discussed in Sec. 4.4. EC1-2 is characterized by the approximately largest Hs, which are important to the responses of tilt/pitch angle and nacelle surge acceleration. EC1–3 and EC1–4 have large Tp, which are closer to the natural

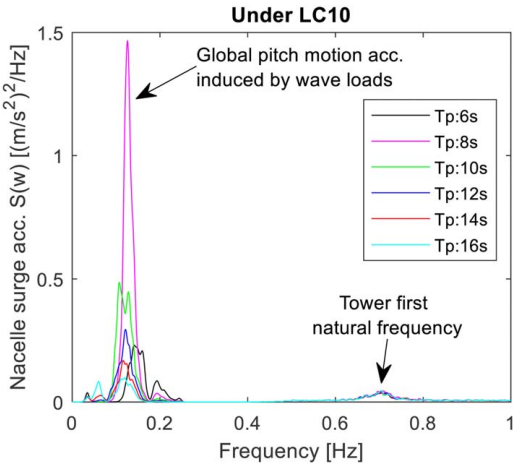

Fig. 8 Power spectra of nacelle surge acceleration for different Tp under LC10, considering first-order wave loads only

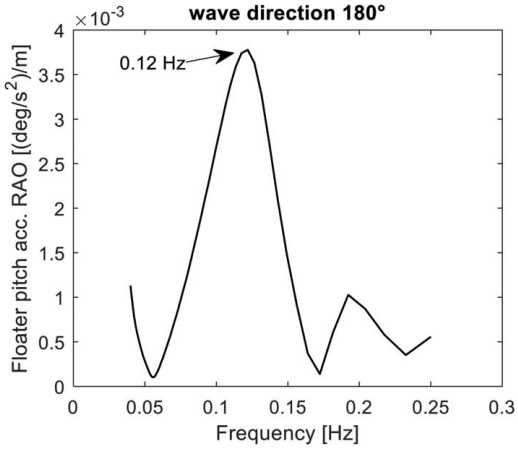

Fig. 9 RAOS of the floater pitch accelerations

period of global pitch motion. Significant responses in tilt/pitch angle and nacelle surge acceleration might occur at the large Tp conditions near the resonance.

Turbulent wind, irregular waves, and simulation time are modeled and conducted consistently with the description in Sec. 4.1. Under all simulation conditions, wind and waves are aligned in the 180 deg direction, as illustrated in Fig. 2. The selection of the 180 deg direction for the SLS assessment is based on the identification of the critical direction in the intact stability study of Li et al. [1] since the floater tilt angle studied in this work is closely associated with the intact stability of the FWT. In addition, both the first- and second-order wave loads are considered in all the conditions in this section. Due to the significant time required for the multiple samples and the need to account for statistical uncertainty in extreme values, which are of concern herein, we applied two procedures. First, 18 samples and the Gumbel method are used to predict extremes for several cases accurately. Then, a single sample is considered for other cases to predict the extreme loads via a formula of $\mu + k \cdot \sigma$, which is explained in detail in the next section. The procedure is effective since the uncertainty in mean and standard deviation are smaller than that for the extreme value in a sample. In the present work, 18 wind and wave samples are considered for four representative environmental conditions, which are used to conduct the extreme response analysis in Sec. 5.2.

5.2 Extreme Value Estimation. The type I extreme value distribution, i.e., Gumbel distribution, is used to predict the short-term

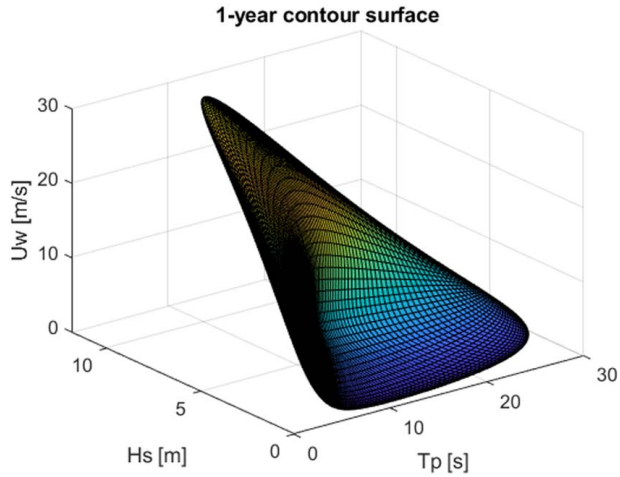

Fig. 10 One-year 3D environmental contour surface:

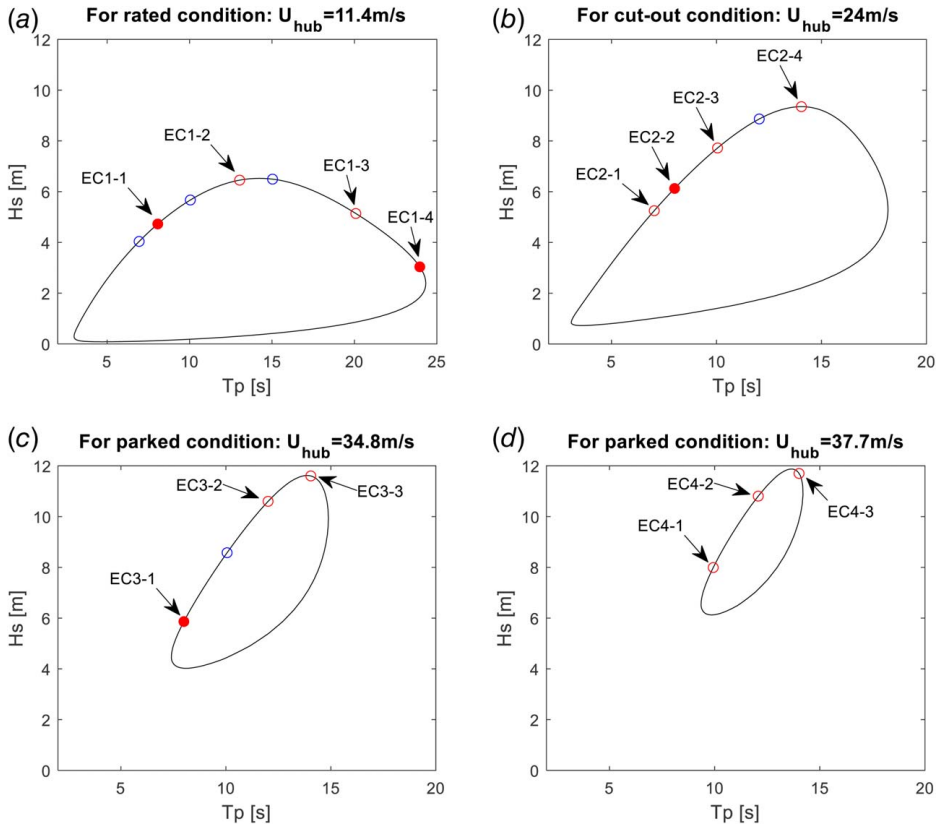

Fig. 11 One-year environmental contour lines for rated, cut-out, and two parked conditions: (*a*) rated condition, (*b*) cut-out condition, (*c*) parked condition 1, and (*d*) parked condition 2

extreme responses. First, short-term dynamic simulations are conducted, and then the maximum value in each sample, is picked for fitting the Gumbel distribution. Afterward, the specific fractiles are used to determine the extrapolated extreme responses. The cumulative Gumbel distribution is expressed by

$$F_{X_e}(x) = \exp\left(-\exp\left(-\frac{x-\mu}{\beta}\right)\right) \tag{3}$$

where $F_{X_e}(x)$ is the Gumbel extreme value distribution; μ and β describe the location and scale parameters, respectively. Equation (1) can be rewritten to form the linear function as follows by using the logarithm

$$-\ln(-\ln(F_{X_e}(x))) = \frac{x}{\beta} - \frac{\mu}{\beta} \tag{4}$$

The parameters μ and β can be estimated by using the least-square fitting method from the cumulative distribution in a probability paper.

Figure 12 shows the prediction of the short-term extreme responses of the floater tilt angle and nacelle surge acceleration by the Gumbel method, where 90% fractile is used to determine the extreme values. The environmental conditions of EC2–2 are taken as an example to illustrate the extreme value analysis. In each figure, the Gumbel fitting is based on 18 original data that refer to the 1-h maximum values in 18 simulations with independent wind and wave samples. The R^2 is the coefficient of determination, which is the measure of the performance of data prediction. It is observed that all the R^2 values are very close to 1, which means that the extrapolated extreme responses are quite reliable.

Table 6 shows the estimated extreme responses of floater tilt/pitch angles and nacelle surge accelerations, respectively, at the 90% fractile of the Gumbel distribution under the four environmental conditions. Inspired by the analytical expression for the expected maximum (most probable maximum) for a Gaussian process, the extreme value of the response corresponding to 90% is estimated by the formula of $\mu + k \cdot \sigma$, where the k value is a multiplying factor that is approximately equal to 4 for the most probable extreme value. For the Gaussian process, the extreme value is proportional to $(\ln N)^{0.5}$, where N is the number of individual maxima. Based on the estimated extreme values by the Gumbel method and the ensemble average of mean values and standard deviations, the k values for the two responses are calculated. In general, certain differences exist for the k values estimated based on the Gumbel method and the reference value 4, especially for nacelle surge acceleration under EC1–4. This is mainly due to the following reasons:

Table 5 Environmental conditions for the case study

Sample no.	Envir. condition	U_{10m} (m/s)	U_{hub} (m/s)	T_I	Hs (m)	Tp (s)
20	EC1–1	7.86	11.4	0.149	4.73	8.07
1	EC1–2	7.86	11.4	0.149	6.45	13.04
1	EC1–3	7.86	11.4	0.149	5.14	20.09
20	EC1–4	7.86	11.4	0.149	3.04	23.97
1	EC2–1	16.55	24.0	0.118	5.25	7.03
20	EC2–2	16.55	24.0	0.118	6.13	8.00
1	EC2–3	16.55	24.0	0.118	7.72	10.05
1	EC2–4	16.55	24.0	0.118	9.35	14.05
20	EC3–1	24.00	34.8	0.109	5.86	8.00
1	EC3–2	24.00	34.8	0.109	10.60	12.01
1	EC3–3	24.00	34.8	0.109	11.60	14.04
1	EC4–1	26.00	37.7	0.108	7.99	9.93
1	EC4–2	26.00	37.7	0.108	10.81	12.07
1	EC4–3	26.00	37.7	0.108	11.70	14.01
1	EC5	31.20	45.2	0.112	15.40	14.50

Note: The 10-min wind speed at the hub is 1.45 times the 1-hour wind speed at 10 m based on IEC 61400-3 [16] and DNVGL-ST-0437 [3].

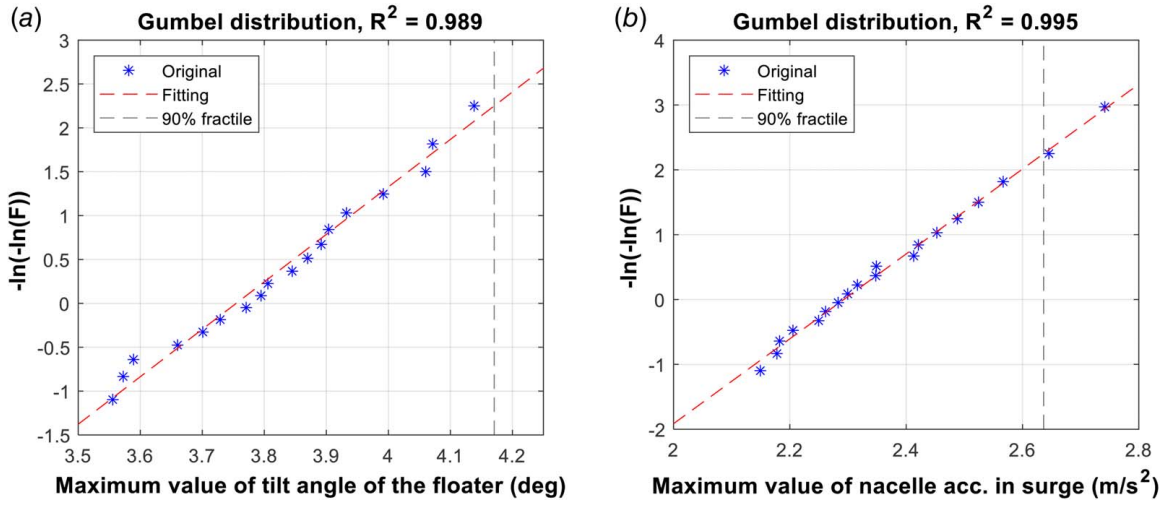

Fig. 12 Estimation of extreme values of the floater tilt angle and nacelle surge acceleration under the EC2–2 condition

(1) the extreme value is estimated at 90% fractile in the Gumbel method instead of the fractile for the most probable value; (2) the statistical responses are not narrow band processes; (3) the average period is relatively small for the high-frequency signal, which leads to the large value of N; (4) the response process deviates from a Gaussian process. This deviation can be measured by the skewness and kurtosis of the distributions, which are 0 and 3, respectively, for the Gaussian process. Table 6 shows the skewness and kurtosis values of the floater tilt angle and nacelle surge acceleration, respectively. Certain differences are observed from the reference values of the Gaussian distribution, which implies that non-Gaussianity exists in the responses. This might be caused by the nonlinear load effects, such as wind and wave viscous drag forces on the tower and floater, respectively.

5.3 Serviceability Limit States Assessment for the Case Study. Table 7 shows response statistics of the floater tilt/pitch angel and nacelle accelerations under environmental conditions in Table 5 based on a single sample of 1 h. Comparing the mean values and standard deviations under EC1–1, EC1–4, EC2–2, and EC3–1 between cases of ensemble average of 20 samples in Table 6 and a single sample in Table 7, a small influence due to the stochastic uncertainty is observed. The extreme values are estimated based on the simplified analytical method by the formula of $\mu + k \cdot \sigma$, where k values estimated under EC1–1, EC1–4, EC2–2, and EC3–1 in Table 3 are used in other conditions.

For the floater tilt/pitch angle, in the normal operating conditions from EC1–1 to EC2–4, the most significant responses occur in the rated condition. For the given mean wind speed at the hub for rated condition, different combinations of Hs and Tp of annual occurrence do not influence the floater tilt/pitch angle significantly, which implies that wind loads dominate. In the parked conditions from EC3–1 to EC4–3, larger floater tilt/pitch responses generally appear at conditions with larger U_{hub} and Hs, where wind drag force on the tower and wave loads mainly contribute to the mean values and standard deviations, respectively.

For the nacelle surge acceleration, in all the conditions of normal operating and parked, significant response occurs at the environmental conditions with critical Tp where RAO peak of floater pitch acceleration is located. This is because floater pitch acceleration significantly contributes to the nacelle surge acceleration due to large tower height, as discussed in Sec. 4.

In this case study, both floater tilt/pitch angle and nacelle surge acceleration satisfy the SLS criteria, as described in Sec. 2. For the tilt/pitch angle, a design check can be carried out only based on the rated condition. In the parked condition, the extreme values are far less than the criterion of 15 deg. For the design check of nacelle surge acceleration, the main attention should be placed on the cut-out condition, since the combination of large wind turbulence, large Hs and critical Tp result in significant responses. Although wind loads contribute to the nacelle surge accelerations, which is mainly due to the variations of wind loads rather than the mean values. This can be explained by Fig. 4(*b*) where STD of nacelle surge accelerations increases with mean wind speeds from 8 m/s to 24 m/s under "only wind" conditions. As the mean wind speed increases, wind turbulence increases while mean wind loads decrease due to the control effect.

Although large responses of nacelle surge acceleration also occur in the parked conditions, a large safety tolerance exists due to the large allowable value, 0.6 g, of the design criterion.

Table 6 Estimated extreme values of floater tilt angle and nacelle surge acceleration at 90% fractile of the gumbel distribution, and the derived multiplying factor, *k*, under the four conditions (based on 18 samples of 1 h)

Environmental condition	Structures	Unit	Ensemble average				90% Fractile	
			Mean	STD	Skewness	Kurtosis	Extreme	k
EC1–1	Floater tilt angle	deg	3.37	0.97	−0.03	3.20	6.87	3.60
	Nacelle surge acc.	m/s^2	0	0.44	−0.01	3.04	1.99	4.48
EC1–4	Floater tilt angle	deg	3.50	1.01	0.01	3.30	7.55	4.03
	Nacelle surge acc.	m/s^2	0	0.17	0.05	3.32	1.11	6.39
EC2–2	Floater tilt angle	deg	1.61	0.70	−0.18	3.03	4.17	3.64
	Nacelle surge acc.	m/s^2	0	0.59	0.01	3.02	2.64	4.44
EC3–1	Floater tilt angle	deg	0.39	0.67	−0.19	3.13	2.77	3.56
	Nacelle surge acc.	m/s^2	0	0.55	−0.02	3.06	2.19	3.98

Table 7 Response statistics of floater tilt/pitch and nacelle surge accelerations under different environmental conditions based on a single sample of 1 h

	Tilt/pitch angle (deg)			Nacelle surge acc. (m/s^2)	
Load case	Mean	STD	Extreme	STD	Extreme
EC1–1	3.37	0.94	6.75	0.44	1.97
EC1–2	3.45	0.97	7.36	0.21	1.34
EC1–3	3.48	0.95	7.31	0.14	0.89
EC1–4	3.49	0.94	7.28	0.18	1.15
EC2–1	1.66	0.65	4.03	0.17	0.75
EC2–2	1.63	0.71	4.21	0.58	2.58
EC2–3	1.66	0.82	4.64	0.25	1.11
EC2–4	1.75	0.76	4.52	0.30	1.33
EC3–1	0.39	0.69	2.85	0.54	2.15
EC3–2	0.39	0.99	3.91	0.35	1.39
EC3–3	0.44	0.94	3.79	0.37	1.47
EC4–1	0.51	0.88	3.64	0.26	1.03
EC4–2	0.52	1.03	4.19	0.36	1.43
EC4–3	0.57	0.96	3.99	0.38	1.51
EC5	0.88	1.38	5.79	0.67	2.67

Note: The k values are determined as follows: For cases EC1–1 (based on EC1–1 in Table 6); for cases EC1–2,3,4 (based on EC1–4 in Table 6); for cases EC2-i (based on EC2–2 in Table 6); for cases EC3,4,5–i (based on EC3–1 in Table 6).

6 Concluding Remarks

This paper deals with the principles of serviceability limit state (SLS) assessment and their application for a 10-MW semi-submersible floating wind turbine (FWT). As a research work, this paper focus on presenting the methods, procedure, and criteria for FWT serviceability assessment, which intends to provide a basis for serviceability analysis since very limited information exists in design standards. An overview of possible serviceability criteria for FWTs is presented, with a focus on floater tilt angle and nacelle accelerations which relate to power production. Static and dynamic characteristics of the tilt angle and nacelle acceleration responses are investigated for wind turbine models with different fidelities and under different wind and wave conditions. In addition, an efficient procedure for SLS assessment is proposed and applied to the case study. The main findings are summarized as follows:

- The 10-MW semi-submersible FWT model in the present work satisfies the serviceability criteria in terms of the floater tilt angles and nacelle surge accelerations. Normal operating conditions are more critical for the SLS design checks than the parked condition because of the large tolerance to the serviceability requirement for the parked condition.
- Wave spectra peak period (Tp) has a significant influence on nacelle surge accelerations because of the close link with the global rigid-body pitch accelerations. Response amplitude operator analysis of the global pitch accelerations should be conducted to identify the critical Tp for serviceability limit state assessment. Attention should be devoted to cut-out conditions in terms of the assessment of nacelle surge accelerations.
- Only the rated condition needs to be considered for the assessment of the tilt/pitch angle of the floater because the response is dominated by wind loads.
- In normal operating conditions, the floater tilt angle is mainly caused by wind excitation loads and global pitch motion resonance induced by low-frequency turbulent wind loads. The nacelle surge acceleration is mainly due to the wave loads and global rigid-body pitch acceleration induced by wave loads. The nacelle pitch acceleration (the response is very small) is mainly contributed by the tower's second vibration resonance induced by wind loads. In the parked condition, the floater tilt angle response is mainly caused by wave excitation. Both the nacelle surge and pitch accelerations are mainly caused by the wave loads and global rigid-body pitch accelerations induced by wave loads.
- The mean tilt angle estimated through dynamic analysis with the fully integrated model is about 30% smaller than that calculated by the static analysis for the free-floating model. Different controller systems lead to different rotor thrust forces between the land-based reference wind turbine and FWT. Using the rotor thrust force of the land-based turbine for a floater design will result in a conservative serviceability performance check for the present system. In addition, second-order wave loads make the standard deviation of tilt/pitch angle and nacelle surge acceleration increase by around 10% and 3–6%, respectively.

Overall, this study illustrates a comprehensive procedure for serviceability performance analysis of semi-submersible FWTs. The dynamic characteristics of the relevant static and stochastic wave- and wind-induced responses for serviceability limit states are studied in depth. Target values for the limit state criteria are briefly discussed. It is believed that the present work provides a first step towards establishing improved design standards and engineering practices. On the basis of this work, future research should be conducted to further clarify the specific serviceability criteria and to establish connections between serviceability and safety criteria, also relating, for instance, to clearance requirements. One interesting work will be investigating the influence of floater design on nacelle surge acceleration and then on drivetrain safety of the 10-MW turbine based on the present work and authors' previous studies [17–20] in relation to drivetrain analysis.

A most important issue is to critically assess the criteria by the actual physical response, in view of the fact that the effect of tilt angle and nacelle accelerations should be accounted for in the load effect analysis and the criteria to avoid inserviceability and failure. Finally, the serviceability performance investigated in this study is made without considering faults. Further assessment of the relevance of considering fault conditions is needed.

Acknowledgement

The authors would like to acknowledge the financial support from PowerChina HuaDong Engineering Corporation Limited, Hangzhou Zhejiang China, 311122 (No. 90814100/642005). In addition, the second author would like to acknowledge the support from the National Natural Science Foundation of China (NSFC) (Grant No. 52250710156) and from the Faculty of Maritime and Transportation, Ningbo University, Ningbo, China.

Conflict of Interest

There are no conflicts of interest.

Data Availability Statement

The datasets generated and supporting the findings of this article are obtainable from the corresponding author upon reasonable request.

References

[1] Li, W., Wang, S., Moan, T., Gao, Z., and Gao, S., 2023, "Global Design Methodology for Semi-Submersible Hulls of Floating Wind Turbines," Preprint in Renewable Energy, https://papers.ssrn.com/sol3/papers.cfm?abstract_id=4455440.

[2] DNVGL, 2016, *DNVGL-ST-0126: Support Structures for Wind Turbines*, DNV GL, Oslo, Norway.

[3] DNV GL, 2016, DNVGL-ST-0437: Loads and Site Conditions for Wind Turbines, DNV GL, Oslo, Norway.

[4] Nejad, A. R., Bachynski, E. E., and Moan, T., 2019, "Effect of Axial Acceleration on Drivetrain Responses in a Spar-Type Floating Wind Turbine," ASME J. Offshore Mech. Arct. Eng., **141**(3), p. 031901.

[5] IEC-TS-61400-3-2, 2019, IEC TS 61400-3-2: 2019 Wind Energy Generation Systems-Part 3-2: Design Requirements for Floating Offshore Wind Turbines.

[6] DNV, 2021, "DNVGL-ST-0119: Floating Wind Turbine Structures (Edition June 2021)," Technical Report. http://www.dnvgl.com.

[7] Yu, W., Müller, K., Lemmer, F., Schlipf, D., Bredmose, H., Borg, M., Landbø, T., and Andersen, H., 2018, *LIFES50+ D4. 2: Public Definition of the two LIFES50+ 10 MW Floater Concepts,* University of Stuttgart, Deliverable Report.
[8] Luan, C., Gao, Z., and Moan, T., 2016, "Design and Analysis of a Braceless Steel 5-MW Semi-Submersible Wind Turbine," Proceedings of the International Conference on Offshore Mechanics and Arctic Engineering, American Society of Mechanical Engineers, p. V006T009A052.
[9] Wang, S., Moan, T., and Gao, Z., 2022, "Conceptual Global Design of Semi-Submersible Hulls for Floating Wind Turbines," Technical Report No. 90814100/642002, Prepared for Power China. Department of Marine Technology, NTNU, Nov. 9, 2022. (Confidential).
[10] Wang, S., Moan, T., and Gao, Z., 2023, "Methodology for Global Structural Load Effect Analysis of the Semi-Submersible Hull of Floating Wind Turbines Under Still Water, Wind, and Wave Loads," Mar. Struct., **91**, p. 103463.
[11] Faltinsen, O., 1993, *Sea Loads on Ships and Offshore Structures*, Part of Cambridge Ocean Technology Series, Cambridge University Press.
[12] Zeng, X., Shi, W., Feng, X., Shao, Y., and Li, X., 2023, "Investigation of Higher-Harmonic Wave Loads and Low-Frequency Resonance Response of Floating Offshore Wind Turbine Under Extreme Wave Groups," Mar. Struct., **89**, p. 103401.
[13] Li, L., Gao, Z., and Moan, T., 2015, "Joint Distribution of Environmental Condition at Five European Offshore Sites for Design of Combined Wind and Wave Energy Devices," ASME J. Offshore Mech. Arct. Eng., **137**(3), p. 030901.
[14] Wang, S., Moan, T., and Jiang, Z., 2022, "Influence of Variability and Uncertainty of Wind and Waves on Fatigue Damage of a Floating Wind Turbine Drivetrain," Renew. Energy, **181**, pp. 870–897.
[15] Wang, S., Xing, Y., Balakrishna, R., Shi, W., and Xu, X., 2023, "Design, Local Structural Stress, and Global Dynamic Response Analysis of a Steel Semi-Submersible Hull for a 10-MW Floating Wind Turbine," Eng. Struct., **291**, p. 116474.
[16] IEC61400-3, 2009, *IEC 61400-3 Wind Turbines Part3: Design Requirements for Offshore Wind Turbines*, International Electrotechnical Commission, Geneva, Switzerland.
[17] Wang, S., Moan, T., and Nejad, A. R., 2021, "A Comparative Study of Fully Coupled and De-Coupled Methods on Dynamic Behaviour of Floating Wind Turbine Drivetrains," Renew. Energy, **179**, pp. 1618–1635.
[18] Wang, S., Nejad, A., Bachynski, E. E., and Moan, T., 2021, "A Comparative Study on the Dynamic Behaviour of 10 MW Conventional and Compact Gearboxes for Offshore Wind Turbines," Wind Energy, **24**(7), pp. 770–789.
[19] Wang, S., Nejad, A. R., Bachynski, E. E., and Moan, T., 2020, "Effects of Bedplate Flexibility on Drivetrain Dynamics: Case Study of a 10 MW Spar Type Floating Wind Turbine," Renew. Energy, **161**, pp. 808–824.
[20] Wang, S., Nejad, A. R., and Moan, T., 2020, "On Design, Modelling, and Analysis of a 10-MW Medium-Speed Drivetrain for Offshore Wind Turbines," Wind Energy, **23**(4), pp. 1099–1117.